Ground-state hyperfine splitting for Rb, Cs, Fr, Ba^+, and Ra^+

J. S. M. Ginges,[1] A. V. Volotka,[2] and S. Fritzsche[2,3]
[1]*Centre for Engineered Quantum Systems, School of Physics, The University of Sydney, Sydney NSW 2006, Australia*
[2]*Helmholtz-Institut Jena, Fröbelstieg 3, D-07743 Jena, Germany*
[3]*Theoretisch-Physikalisches Institut, Friedrich-Schiller-Universität Jena, Max-Wien-Platz 1, D-07743 Jena, Germany*
(Received 22 September 2017; published 12 December 2017)

We have systematically investigated the ground-state hyperfine structure for alkali-metal atoms ^{87}Rb, ^{133}Cs, and ^{211}Fr and alkali-metal-like ions $^{135}Ba^+$ and $^{225}Ra^+$, which are of particular interest for parity violation studies. The quantum electrodynamic one-loop radiative corrections have been rigorously evaluated within an extended Furry picture employing core-Hartree and Kohn-Sham atomic potentials. Moreover, the effect of the nuclear magnetization distribution on the hyperfine structure intervals has been studied in detail and its uncertainty has been estimated. Finally, the theoretical description of the hyperfine structure has been completed with full many-body calculations performed in the all-orders correlation potential method.

DOI: 10.1103/PhysRevA.96.062502

I. INTRODUCTION

It has become apparent in the last decade that quantum electrodynamic (QED) radiative corrections may give sizable contributions to properties of heavy atoms. Notably, QED radiative corrections to the parity violating electric dipole amplitude in Cs were critical in restoring the deviation of the measured value of the nuclear weak charge from the value predicted by the standard model of particle physics [1–10]. Indeed, it has been shown that QED radiative corrections may contribute at the level (0.1–1)% to s-p energy intervals [9,11–16], usual E1 amplitudes [9,15,17,18], hyperfine structure intervals [19,20], and parity violating amplitudes [7–9,15,18] for heavy alkali-metal atoms and near-neutral alkali-metal-like ions.

The current work is motivated by a new generation of atomic parity violation experiments that are underway or in preparation for Cs [21], Fr [22–24], Ba^+ [25,26], and Ra^+ [27]. Rb has also been promoted as a candidate for such studies [28]. Single-isotope measurements of (nuclear spin-independent) atomic parity violation are sensitive to the nuclear weak charge, which is based on a unique combination of coupling constants, and complement collider-based studies [29–31].

Clean interpretation of single-isotope measurements depends on the ability to calculate the atomic parity violating amplitudes to high accuracy. The highest accuracy has been reached for Cs, with a claimed uncertainty within 0.5% [9,32–34]. It is possible to sidestep atomic theory by performing measurements along an isotope chain and taking ratios of measured values [35]. This approach, however, probes a different combination of coupling constants than probed in single-isotope studies, and the latter studies thus remain valuable in providing unique information about particle physics [36,37].

In the current work, we calculate the ground-state hyperfine structure for atoms of interest for parity violation measurements. The hyperfine structure depends on the electronic wave functions close to the nucleus, and comparison between theory and experiment allows the quality of the wave functions in this region to be gauged. This comparison, along with those for electric dipole transition amplitudes and energy intervals, forms part of the error analysis for parity violation calculations (see, e.g., Refs. [32,33]). In order to make a meaningful comparison for the hyperfine structure, however, one first needs to separate out all other effects. In particular, the QED radiative and the nuclear magnetization distribution effects need to be accounted for before an assessment of the quality of the many-electron wave functions may be made. In this paper we address this need.

The only rigorous QED calculations of the ground-state hyperfine structure for heavy alkali-metal atoms have been performed by Sapirstein and Cheng [19], and there are no such data for the alkali-metal-like ions. Sapirstein and Cheng used the Kohn-Sham approximation to model the atomic potential. In the current work, we perform rigorous QED calculations in two local atomic potentials, Kohn-Sham and core-Hartree, applied to the ground-state hyperfine structure for ^{87}Rb, ^{133}Cs, ^{211}Fr, $^{135}Ba^+$, and $^{225}Ra^+$. We also investigate in the current work the nuclear magnetization distribution effect—the so-called Bohr-Weisskopf effect—within different nuclear models for these systems. It is common practice in many-body calculations of the hyperfine structure for heavy atoms to adopt the model of the uniformly magnetized sphere. The validity of this model, however, is not well motivated for odd-nucleon nuclei in particular, and different magnetization models may give significantly different results. For example, we observe a very sizable correction (0.5%) to the hyperfine structure for ^{133}Cs when using a single-particle model for the nuclear magnetization distribution rather than the sphere. To complete the theoretical study of the hyperfine structure, we perform state-of-the-art many-body calculations in the all-orders correlation potential method.

This paper is organized as follows. In Sec. II, we determine the zeroth-order hyperfine intervals in core-Hartree and Kohn-Sham potentials. Our calculations of QED radiative corrections are presented in Sec. III. We discuss different magnetization models and calculate their effects in Sec. IV. In Sec. V, we present results of our many-body calculations, and give a complete theoretical description of the hyperfine intervals. The results are discussed in Sec. VI and concluding remarks given in Sec. VII.

II. THE HYPERFINE INTERVAL

The magnetic interaction of an atomic electron with the magnetic dipole moment of the nucleus is given by

$$h_{\rm hfs} = |e|\boldsymbol{\alpha}\cdot\mathbf{A}(\mathbf{r}) = \frac{|e|}{4\pi}\frac{\boldsymbol{\mu}\cdot(\mathbf{r}\times\boldsymbol{\alpha})}{r^3}F(r), \qquad (1)$$

where $\boldsymbol{\alpha}$ is a Dirac matrix, $\mathbf{A}$ is the vector potential of the nucleus, $\boldsymbol{\mu} = \mu\mathbf{I}/I$ is the nuclear magnetic moment, and $\mathbf{I}$ is the nuclear spin. We use relativistic units $c = \hbar = m = 1$, $e^2/(4\pi) = \alpha$ throughout unless otherwise stated. The factor $F(r)$ models the magnetization distribution, and for a point nucleus $F(r) = 1$.

We consider the hyperfine splitting in the ground states of alkali-metal atoms and alkali-metal-like ions. The hyperfine interaction Eq. (1) splits the state $^2S_{1/2}$ into two levels $I \pm 1/2$. The interval between the levels in the zeroth-order approximation—with local atomic potential and point-nucleus magnetization—is given by

$$\nu^{(0)} = \frac{2}{3}\frac{\alpha^2}{m_p} g_I (2I+1) \int_0^\infty dr\, G_a(r) F_a(r)/r^2. \quad (2)$$

Here, $G_a(r)$ and $F_a(r)$ are the upper and lower radial components of the Dirac single-electron wave function φ_a that satisfies the Dirac equation in the extended Furry representation,

$$(\boldsymbol{\alpha}\cdot\mathbf{p} + \beta + V_{\rm nuc}(r) + V_{\rm scr}(r))\varphi_a = \epsilon_a \varphi_a; \quad (3)$$

β is a Dirac matrix, $V_{\rm nuc}(r)$ is the nuclear potential, and $V_{\rm scr}(r)$ is the local screening (electronic) potential that partially accounts for the interaction between the valence electron and the closed core electrons. For $V_{\rm scr}$, in calculations of the QED corrections, we use the core-Hartree (CH) potential and the Kohn-Sham (KS) potential derived within density-functional theory [38].

In the core-Hartree approach, the $N-1$ core electrons are solved self-consistently in the direct potential formed from the core,

$$V_{\rm CH}(r) = \alpha \int_0^\infty dr' \frac{\rho_{\rm c}(r')}{r_>}, \quad (4)$$

where $r_> = \max(r,r')$ and $\rho_{\rm c}(r) = \sum_b (G_b^2(r) + F_b^2(r))$ is the charge density of the core electrons b, $\int_0^\infty dr \rho_{\rm c}(r) = N-1$. The valence electron wave functions are found in this potential. In the Kohn-Sham approach [38], an approximation for the exchange potential is included,

$$V_{\rm KS}(r) = \alpha \int_0^\infty dr' \frac{\rho_{\rm t}(r')}{r_>} - \frac{2}{3}\frac{\alpha}{r}\left[\frac{81}{32\pi^2} r\rho_{\rm t}(r)\right]^{1/3}, \quad (5)$$

where $\rho_{\rm t}$ is the total (core and valence) electron density $\rho_{\rm t} = \rho_{\rm c} + (G_a^2(r) + F_a^2(r))$, and the self-consistency procedure is carried out in the potential formed from all electrons. In the KS approach, the correct asymptotic form of the atomic potential at large distances, $V_{\rm nuc} + V_{\rm KS} = -\alpha/r$, is enforced using the Latter correction [39].

We use a finite nuclear charge potential $V_{\rm nuc}(r)$ at all stages of our calculations, with charge density corresponding to the two-parameter Fermi distribution,

$$\rho_{\rm nuc}(r) = \frac{\rho_0}{1 + \exp[(r-c)/a]}. \quad (6)$$

The thickness parameter $t = a(4\ln 3)$ is taken to be $t = 2.3$ fm for all nuclei and the half-density radius c is found from the root-mean-square radius $r_{\rm rms}$ compiled in Ref. [40], $c^2 \approx (5/3)r_{\rm rms}^2 - (7/3)(\pi a)^2$. The isotopes we consider in this work with associated nuclear radii $r_{\rm rms}$ and nuclear moments μ, spin I, and parity π—from Ref. [41]—are presented in Table I.

TABLE I. Nuclear parameters used in this work: root-mean-square radii $r_{\rm rms}$ in units fm, magnetic moments in units μ_N, and spin and parity I^π.

	^{87}Rb	^{133}Cs	^{135}Ba	^{211}Fr	^{225}Ra
$r_{\rm rms}$	4.1989	4.8041	4.8294	5.5882	5.7150
μ	2.751818(2)	2.582025(3)	0.838627(2)	4.00(8)	−0.7338(15)
I^π	$3/2^-$	$7/2^+$	$3/2^+$	$9/2^-$	$1/2^+$

We parametrize the finite-nucleus magnetization and QED radiative corrections to the hyperfine structure intervals as

$$\nu = \nu^{(0)}\left(1 + \frac{\alpha}{\pi}F^{\rm BW} + \frac{\alpha}{\pi}F^{\rm QED}\right). \quad (7)$$

The finite-nucleus magnetization correction—the Bohr-Weisskopf (BW) effect [42]—is expressed in terms of a relative correction $F^{\rm BW}$, and $F^{\rm QED}$ is the relative QED radiative correction comprising the vacuum polarization and self-energy, $F^{\rm QED} = F^{\rm VP} + F^{\rm SE}$.

Our zeroth-order results $\nu^{(0)}$ in core-Hartree and Kohn-Sham approximations alongside the values of Sapirstein and Cheng [19] are presented in Table II. Our Kohn-Sham results agree precisely with those of Ref. [19] when we take the same nuclear parameters (nuclear charge radii, nuclear moments) used in that work. The spread in core-Hartree and Kohn-Sham values for $\nu^{(0)}$ for the considered systems is within 3%.

III. QED RADIATIVE CORRECTIONS

The one-loop QED contributions to the hyperfine splitting incorporate the self-energy and vacuum polarization corrections. While there are a number of *ab initio* QED calculations of these corrections for hydrogenlike, lithiumlike, and boronlike ions (see, e.g., [43]), there are only a few works devoted to the case of neutral heavy atoms. The latter were performed by Sapirstein and Cheng in alkali-metal atoms for s states in Ref. [19], for $p_{1/2}$ states in Ref. [44], and for $p_{3/2}$ states in Ref. [20]. Calculations of QED corrections in neutral atoms must account for electron screening effects from the very beginning. Thus, in contrast to highly charged

TABLE II. Zeroth-order hyperfine structure intervals $\nu^{(0)}$ for the ground states of Rb, Cs, Ba^+, Fr, and Ra^+ in core-Hartree and Kohn-Sham potentials. Units are in MHz.

	$\nu^{(0)}$		
	CH	KS	KS[a]
^{87}Rb	4956.04	4886.78	4886.320
^{133}Cs	6156.85	6164.90	6164.831
$^{135}Ba^+$	5652.21	5675.51	–
^{211}Fr	27023.9	27545.4	27244.2[b]
$^{225}Ra^+$	−20590.1	−21128.2	–

[a]Reference [19].

[b]From Ref. [19] obtained with isotope ^{212}Fr and adjusted for different μ.

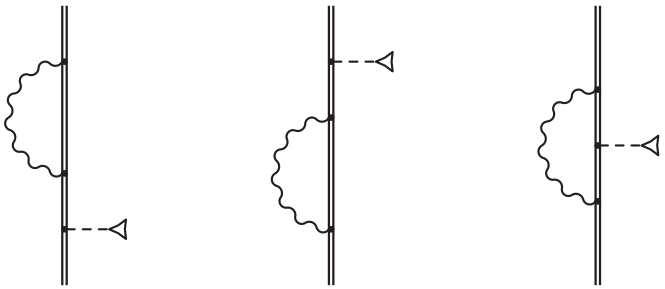

FIG. 1. Feynman diagrams representing the self-energy correction to the hyperfine splitting. The wavy line indicates the photon propagator and the double line indicates the bound-electron wave functions and propagators in the effective potential comprising the Coulomb and screening potentials. The dashed line terminated with the triangle denotes the hyperfine interaction.

ions where one can use the pure Coulomb potential as the zeroth-order approximation (the original Furry picture), for neutral atoms the calculations begin with a local screening potential (the extended Furry picture). In this work we employ the core-Hartree and Kohn-Sham potentials, Eqs. (4) and (5), respectively. In this section we evaluate the self-energy and vacuum polarization corrections within the extended Furry representation for the hyperfine structure intervals for the ground states of Rb, Cs, Ba^+, Fr, and Ra^+.

The complete gauge invariant set of diagrams that need to be considered are shown in Figs. 1 and 2 for the self-energy and vacuum polarization corrections, respectively. The formal expressions for these diagrams from the first principles of QED are derived by employing the two-time Green's function method [45]. The correction due to the self-energy diagrams may be written as

$$\nu^{\rm SE} = 2\sum_{n}^{\varepsilon_n\neq\varepsilon_a}\frac{\langle a|T_0|n\rangle\langle n|\Sigma(\varepsilon_a)|a\rangle}{\varepsilon_a-\varepsilon_n}+\langle a|\frac{d\Sigma(\varepsilon)}{d\varepsilon}\bigg|_{\varepsilon=\varepsilon_a}|a\rangle\langle a|T_0|a\rangle + \frac{i}{2\pi}\int_{-\infty}^{\infty}d\omega\sum_{n_1n_2}\frac{\langle an_2|I(\omega)|n_1a\rangle\,\langle n_1|T_0|n_2\rangle}{(\varepsilon_a-\omega-\varepsilon_{n_1}u)(\varepsilon_a-\omega-\varepsilon_{n_2}u)}, \tag{8}$$

where the first term is the so-called *irreducible* part, the second is the *reducible*, and the third one is the *vertex* contribution. The self-energy operator $\Sigma(\varepsilon)$, its derivative $d\Sigma(\varepsilon)/d\varepsilon$, the interelectronic-interaction operator $I(\omega)$, and the hyperfine operator T_0 are defined in a similar way as in Refs. [46–48], and $u = 1 - i0$ preserves the proper treatment of poles of the electron propagators. The self-energy corrections given by Eq. (8) suffer from ultraviolet divergences. In order to cancel these divergences explicitly we have employed the standard renormalization scheme, details of which may be found, e.g., in Ref. [49]. The infrared divergences which occur in the reducible and vertex terms are regularized by introducing a nonzero photon mass and are canceled analytically.

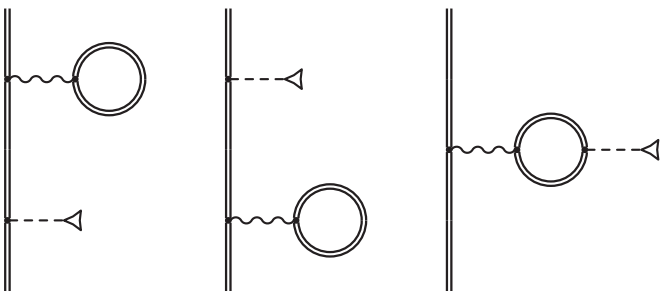

FIG. 2. Feynman diagrams representing the vacuum polarization correction to the hyperfine splitting. Notations are the same as in Fig. 1.

Now let us turn to the vacuum polarization correction to the hyperfine splitting. The corresponding diagrams are depicted in Fig. 2 and provide the following contribution,

$$\nu^{\rm VP} = 2\sum_{n}^{\varepsilon_n\neq\varepsilon_a}\frac{\langle a|T_0|n\rangle\langle n|U_{\rm VP}^{\rm el}|a\rangle}{\varepsilon_a-\varepsilon_n}+\langle a|U_{\rm VP}^{\rm ml}|a\rangle, \tag{9}$$

where the first term is the *electric-loop* part and the second is the *magnetic-loop* contribution. The electric-field-induced $U_{\rm VP}^{\rm el}$ and the magnetic-field-induced $U_{\rm VP}^{\rm ml}$ vacuum polarization potentials are defined in a similar way as in Ref. [50]. In order to regularize the ultraviolet divergence terms one has to decompose these potentials into the Uehling and the Wichmann-Kroll parts. Only the Uehling part contains the divergent terms, and these may be completely removed using the standard renormalization procedure [49]. In this work we have rigorously evaluated the Uehling parts for both the electric- and magnetic-loop contributions. We assume that the ratio of the Uehling and higher-order Wichmann-Kroll terms for neutral atoms remains similar to the case for hydrogenlike ions. Rigorous calculations [51] of the vacuum polarization correction in hydrogenlike ions reveal that the Wichmann-Kroll term increases with nuclear charge and reaches 10% of the Uehling term for the heaviest ions considered ($Z = 83$). Here, we do not account for the Wichmann-Kroll terms, since the uncertainty in the treatment of the screening effects is larger than the estimated contribution of these terms.

In Table III we present our results for the QED radiative corrections to the hyperfine structure intervals. Our calculations were performed for finite nuclear charge (Fermi distribution) and finite nuclear magnetization (uniformly magnetized sphere). Overall our Kohn-Sham results for Rb, Cs, and Fr are in good agreement with the results of Ref. [19]. For the vacuum polarization correction, the small deviation is due to the finite nuclear magnetization effect accounted for in our values. For the case of the self-energy, the calculations are much more involved and the difference can be explained by numerical uncertainties. The QED corrections amount to -0.2% for Rb, -0.4% for Cs and Ba^+, and -0.6% for Fr and Ra^+. The size of these corrections is significant and on the level of correlation uncertainties, as we will see in Sec. V. The variation in results found in CH and KS potentials is within 20%, giving an indication of the sensitivity of QED effects to different treatment of electron screening.

In order to determine the total QED radiative corrections to the hyperfine splitting, we will apply the same relative QED corrections $F^{\rm QED}$ found in the core-Hartree approximation to the final many-body results presented in Sec. V. We estimate the error associated with this scaling procedure using two methods as follows. First, based on the results of rigorous

TABLE III. Relative QED contributions to the hyperfine splitting of the ground states of the neutral atoms ^{87}Rb, ^{133}Cs, and ^{211}Fr and the singly charged ions ^{135}Ba$^+$ and ^{225}Ra$^+$. The vacuum polarization $F^{\rm VP}$, self-energy $F^{\rm SE}$, and QED $F^{\rm QED} = F^{\rm VP} + F^{\rm SE}$ contributions are presented. Our core-Hartree (CH) and Kohn-Sham (KS) results are shown alongside Kohn-Sham results of Ref. [19].

		$F^{\rm VP}$	$F^{\rm SE}$	$F^{\rm QED}$
^{87}Rb	CH	0.729	−1.768	−1.039
	KS	0.746	−1.931	−1.185
	KS[a]	0.765	−1.906	−1.141
^{133}Cs	CH	1.282	−2.920	−1.638
	KS	1.323	−3.229	−1.906
	KS[a]	1.383	−3.201	−1.818
^{135}Ba$^+$	CH	1.305	−2.906	−1.601
	KS	1.332	−3.098	−1.766
^{211}Fr	CH	3.16	−5.75	−2.59
	KS	3.31	−6.43	−3.12
	KS[a]	3.649	−6.248	−2.599
^{225}Ra$^+$	CH	3.15	−5.50	−2.35
	KS	3.25	−5.94	−2.69

[a]Reference [19].

calculations of the screened QED radiative corrections for lithiumlike ions [47,48] compared to results rescaled from core-Hartree values, we conservatively estimate the uncertainty as 50% of the difference between the core-Hartree and rescaled (many-body) results in absolute units. A second estimate of the uncertainty may be given as the difference between core-Hartree and Kohn-Sham results. The uncertainty we assign to the final QED values is the maximum of these estimates.

IV. BOHR-WEISSKOPF CORRECTION

For the magnetization distribution, we employ three different models. The first one is the uniformly magnetized sphere model (sph), where the factor $F(r)$ is given by

$$F(r) = (r/r_n)^3 \tag{10}$$

for $r \leqslant r_n$ and $F(r) = 1$ elsewhere, where $r_n = (5/3)^{1/2}\, r_{\rm rms}$ is the nuclear radius. The other two are the nuclear single-particle models which are widely used for the evaluation of the Bohr-Weisskopf correction [52–54]. Within these models the nuclear magnetization is determined by the total angular momentum of the unpaired proton or neutron. In the first version of this model (SP) we neglect the nucleon spin-orbit interaction and use a homogeneous distribution for the radial part of the nucleon wave function inside the nucleus. In the second version of this model the nucleon spin-orbit interaction is included and the nucleon wave function is found in the Woods-Saxon potential, in a similar way to Ref. [54]. We consider the latter model (SP-WS) to be the most reliable, and we will take the results of this model as our final values for the Bohr-Weisskopf correction. We estimate the uncertainty of our SP-WS results as follows. When the contributions of the nucleon spin and orbital parts are of the same sign, resulting in a relatively large value for $F^{\rm BW,SP-WS}$, the uncertainty is estimated as 30% of this value. When the Bohr-Weisskopf correction,

TABLE IV. Relative BW contributions $F^{\rm BW}$ to the hyperfine splitting of the ground states of the neutral atoms ^{87}Rb, ^{133}Cs, and ^{211}Fr and the singly charged ions ^{135}Ba$^+$ and ^{225}Ra$^+$ calculated in the core-Hartree potential. Results were obtained in three different models of the magnetization distribution, the uniformly magnetized sphere (sph) and single-particle nuclear models (SP and SP-WS).

	$F^{\rm BW,sph}$	$F^{\rm BW,SP}$	$F^{\rm BW,SP-WS}$
^{87}Rb	−1.31	−1.20	−1.23(26)
^{133}Cs	−3.07	−0.89	−0.80(61)
^{135}Ba$^+$	−3.2	−4.4	−5.4(16)
^{211}Fr	−11.6	−5.6	−6.1(23)
^{225}Ra$^+$	−12.1	−12.1	−18.7(56)

evaluated within the model of the uniformly magnetized sphere $F^{\rm BW,sph}$, is larger than that found within the SP-WS model, the uncertainty is assumed to be 20% of $F^{\rm BW,sph}$. To evaluate the Bohr-Weisskopf effect, we use a dense radial grid with radius $110\, a_B$ (a_B is the Bohr radius) and 10^5 grid points. The results for the Bohr-Weisskopf corrections in terms of the $F^{\rm BW}$ factor defined by Eq. (7) are presented in Table IV. Here, we have used the core-Hartree potential.

It is seen from Tables III and IV that the finite-magnetization correction tends to make a larger contribution to the hyperfine intervals than the QED radiative corrections, and this becomes more pronounced for the heavier atoms and ions. Indeed, for ^{87}Rb the Bohr-Weisskopf and QED corrections are of comparable size, while for ^{211}Fr and ^{225}Ra$^+$ the Bohr-Weisskopf corrections reach several times the size of the QED corrections. Moreover, while the sphere model (10) is frequently used in calculations of the hyperfine structure for heavy atoms, it is not the most well-motivated model for odd-nucleon nuclei. Indeed, hyperfine structure measurements along a chain of neutron-deficient isotopes of Fr reveal odd-even staggered results consistent with a simple nuclear single-particle model [55]. For ^{211}Fr, the hyperfine structure result changes by 1.3% when moving from the sphere to the SP-WS model and for ^{133}Cs it changes by 0.5%, a very significant difference on the scale of the error of the correlation calculations, as we will see in Sec. V.

Let us consider the scaling of the relative Bohr-Weisskopf correction in different atomic potentials. For state a, the relative correction is

$$\frac{\alpha}{\pi} F^{\rm BW} = \frac{\int_0^{r_n} dr\, G_a(r) F_a(r) [F(r) - 1]/r^2}{\int_0^{\infty} dr\, G_a(r) F_a(r)/r^2}, \tag{11}$$

where a spherically symmetric magnetization distribution is assumed. The Bohr-Weisskopf effect originates on the nucleus where the electron wave functions satisfy the Dirac equation in the nuclear Coulomb field. For loosely bound valence electrons with binding energies $\ll mc^2, |V_{\rm nuc}|$, such as we consider in this work, the energy dependence is removed and the relativistic radial wave functions for a given angular momentum quantum number κ are the same up to a factor. If the hyperfine interaction were localized within the $1s$ orbit, we would expect the relative Bohr-Weisskopf correction (11) for loosely bound states in different atomic potentials to be very nearly equal. We have evaluated the Bohr-Weisskopf

TABLE V. Results of many-body calculations for the hyperfine structure intervals ν for ^{87}Rb, ^{133}Cs, ^{135}Ba$^+$, ^{211}Fr, and ^{225}Ra$^+$. [The hyperfine interval is related to the magnetic constant A by a factor $(I+1/2)$.] Relativistic Hartree-Fock (RHF), RHF with all-orders correlation potential $\Sigma^{(\infty)}$, and RPA with $\Sigma^{(\infty)}$ results—all with point-nucleus magnetization—are presented in the first rows. The correction from semiempirically adjusting the correlation potential, $f_{\rm exp}\Sigma^{(\infty)}$, is given in the following row. Contributions from structural radiation and normalization ($\delta\Sigma$) and Breit follow. "Subtotal" is the sum of the RPA+$\Sigma^{(\infty)}$ value and the three contributions that follow in the table. QED radiative and Bohr-Weisskopf (BW) corrections found in the single-particle magnetization distribution model (SP-WS) together with their uncertainties are presented in the following rows. Our final theoretical results are presented as "Total". Measured values of the hyperfine intervals and the deviation (Δ) of theory from experiment in absolute units and in % are shown. For the deviation in % we give in the round brackets the uncertainty corresponding to the QED and BW values. For the case of ^{211}Fr, an additional uncertainty associated with the nuclear magnetic moment is presented in the second round brackets. The final digit in the uncertainty given in brackets matches the final digit for the central value. Units are in MHz.

	^{87}Rb	^{133}Cs	^{135}Ba$^+$	^{211}Fr	^{225}Ra$^+$
RHF	4366.1	5734.7	5252.3	29 645	−21 865
RHF+$\Sigma^{(\infty)}$	5762.8	7904.5	6343.5	39 438	−25 703
RPA+$\Sigma^{(\infty)}$	6878.6	9334.8	7424.2	45 824	−29 660
$(f_{\rm exp}-1)\Sigma^{(\infty)}$	45.6	−2.6	−10.2	9	28
$\delta\Sigma$	−95.6	−126.5	−144.3	−624	612
Breit	11.2	23.8	17.0	166	−93
Subtotal	6839.8	9229.5	7286.8	45 374	−29 113
BW	−19.5(42)	−17.0(131)	−91.8(275)	−641(244)	1267(380)
QED	−16.5(23)	−35.1(58)	−27.1(30)	−273(56)	159(23)
Total	6803.8	9177.4	7167.9	44 460	−27 687
Expt.	6834.7[a]	9192.6[a]	7183.3[b]	43 570[c]	−27 731[d]
Δ	−30.9	−15.2	−15.4	890	44
Δ (%)	−0.45(7)	−0.17(16)	−0.21(38)	2.0(6)(20)	−0.2(14)

[a]Reference [58].
[b]Reference [59].
[c]Reference [60].
[d]Reference [61].

corrections within both the core-Hartree and Kohn-Sham potentials and indeed observe an approximate equivalence,

$$F^{\rm BW}_{\rm KS} \approx F^{\rm BW}_{\rm CH}, \tag{12}$$

to within 0.2% for the considered atoms and ions. Furthermore, we have determined the Bohr-Weisskopf correction in both spherical and single-particle SP magnetization models at all levels of many-body approximation (see following section) for ^{133}Cs and found that $F^{\rm BW}$ remains the same to within several 0.1%. Thus, to find the total Bohr-Weisskopf corrections to the hyperfine splitting, we will apply the relative values $F^{\rm BW,SP-WS}$ to the final many-body results presented in the next section.

V. MANY-BODY CALCULATIONS

The hyperfine structure intervals $\nu^{(0)}$ found in the core-Hartree and Kohn-Sham atomic potentials are very much smaller than the measured intervals. For example, for ^{133}Cs the zeroth-order hyperfine interval in core-Hartree and Kohn-Sham is around 6200 MHz, while the measured value is roughly 9200 MHz. This difference is mostly accounted for by many-body effects which we address in the current section.

We perform atomic many-body calculations of the hyperfine structure intervals using the all-orders correlation potential approach [56]. The calculations are carried out for point-nucleus magnetization, and the effects of accounting for finite magnetization distribution are separately considered (see previous section). The many-body approximations and methods we use have been described at length before, and we refer the reader to the review [10] for a more detailed description, diagrams, expressions, and references.

The calculations begin in the relativistic Hartree-Fock (RHF) approximation, where the local electronic potential $V_{\rm scr}(r)$ in the Dirac equation (3) is replaced with the RHF potential,

$$V_{\rm scr} = V^{\rm dir}_{\rm HF} + V^{\rm exch}_{\rm HF}, \tag{13}$$

comprising direct and exchange parts and formed from the $N-1$ core electrons. Expressions for this potential may be found in Ref. [57]. Our RHF values are presented in the first row of results in Table V.

The choice of RHF as the starting approximation simplifies the perturbation theory corrections in the residual Coulomb interaction, with the first nonzero correlation correction appearing in the second order. A second-order nonlocal "correlation potential" $\Sigma^{(2)}(\mathbf{r}_i,\mathbf{r}_j,\epsilon)$ may be constructed, defined such that its averaged value is equal to the second-order correlation correction to the energy, $\delta\epsilon^{(2)} = \langle\varphi|\Sigma^{(2)}|\varphi\rangle$. This potential may be added to the RHF equation to obtain correlation-corrected (Brueckner) wave functions and energies. We go beyond the second order by dressing the Coulomb lines. We do this using the Feynman diagram technique to include important classes of diagrams—electron-electron screening and the hole-particle interaction in hole-particle loops—to all orders in the Coulomb interaction [62]. In this way we obtain an all-orders correlation potential $\Sigma^{(\infty)}(\mathbf{r}_i,\mathbf{r}_j,\epsilon)$ which

is added to the RHF equations (3) with

$$V_{\rm scr} = V_{\rm HF} + \Sigma^{(\infty)} \tag{14}$$

to give Brueckner orbitals $\varphi_{\rm Br}$ and energies $\epsilon_{\rm Br}$. Consideration of correlation-corrected orbitals corresponds to evaluation of the matrix element $\langle\varphi_{\rm Br}|h_{\rm hfs}|\varphi_{\rm Br}\rangle$, and the associated hyperfine intervals are presented in Table V as RHF+$\Sigma^{(\infty)}$.

Note that in obtaining $\Sigma^{(\infty)}$, rigorous calculations are performed for the direct diagrams, while for the smaller exchange diagrams, simplified second-order calculations are carried out. These latter calculations involve a sum over intermediate states. To discretize the states in this sum, we introduce a cavity of radius $40\,a_B$ and diagonalize the relativistic Hartree-Fock Hamiltonian on a set of 40 splines of order $k = 9$ [57]. Higher-order screening corrections are included by introducing multipolarity-dependent electron-electron screening factors found from direct-diagram calculations.

The random-phase approximation (RPA) with exchange (time-dependent Hartree-Fock method) is used to account for polarization of the atomic core by the hyperfine interaction. This leads to an additional term in the hyperfine operator [56],

$$h_{\rm hfs} \to h_{\rm hfs} + \delta V_{\rm hfs}. \tag{15}$$

This term corresponds to a modification of the RHF potential with the hyperfine interaction included in first order in the self-consistency procedure for the core orbitals, $\delta V_{\rm hfs} = \tilde{V}_{\rm HF} - V_{\rm HF}$. We may express the energy shifts due to the hyperfine interaction, including correlations and core polarization, as $\langle\varphi_{\rm Br}|h_{\rm hfs} + \delta V_{\rm hfs}|\varphi_{\rm Br}\rangle$. The corresponding results for the hyperfine intervals are shown in Table V as RPA+$\Sigma^{(\infty)}$.

We use a simple semiempirical means of accounting for missed higher-order correlation corrections. We introduce a factor before the correlation potential,

$$\Sigma^{(\infty)} \to f_{\rm exp}\Sigma^{(\infty)}, \tag{16}$$

that is found by reproducing experimental binding energies in correlation calculations for the energies. This also provides us with a good indication of the error associated with our many-body calculations. These semiempirical corrections are denoted by $(f_{\rm exp} - 1)\Sigma^{(\infty)}$ in Table V.

There are smaller correlation corrections, the "structural radiation," where the hyperfine operator acts on electrons or holes in the internal lines of the correlation potential [56]. We calculate these in the lowest order. As with the exchange part of the correlation potential, we use splined wave functions in a cavity to calculate the structural radiation. At the same level (third-order perturbation theory), there are corrections to the hyperfine intervals arising from normalization of the many-body wave functions [56], $-\langle\varphi|h_{\rm hfs} + \delta V_{\rm hfs}|\varphi\rangle\langle\varphi|\partial\Sigma/\partial\epsilon|\varphi\rangle$. These two corrections are bundled together and denoted by $\delta\Sigma$ in Table V.

We account for the Breit interaction—the magnetic and retardation correction to the Coulomb interaction—in the zero-frequency approximation [57],

$$h_{\rm Breit} = -\frac{\alpha}{2r}(\boldsymbol{\alpha}_i \cdot \boldsymbol{\alpha}_j + \boldsymbol{\alpha}_i \cdot \mathbf{n}\,\boldsymbol{\alpha}_j \cdot \mathbf{n}), \tag{17}$$

where r is the distance between electrons i and j. Calculations are performed at the RPA level, and the Breit corrections to hyperfine intervals are given in Table V.

The contributions described above and tabulated in Table V are summed to give the values "Subtotal". These are our final many-body results, for point-nucleus magnetization and without radiative corrections.

The Bohr-Weisskopf and QED radiative corrections are scaled to the many-body values and presented, along with their uncertainties (as set out in Secs. III and IV), in the following rows. In the final three rows, we give the measured values of the hyperfine intervals and the deviations of our theoretical results from measurements, in MHz and percent.

VI. DISCUSSION

It is seen from Table V that there is reasonable agreement between theoretical and experimental values for all considered elements, with agreement within several 0.1% for ^{87}Rb, ^{133}Cs, and ^{135}Ba$^+$. It is clear, however, that the Bohr-Weisskopf uncertainty—and the nuclear magnetic moment uncertainty for ^{211}Fr—strongly limits testing of the electron wave functions, as we discuss below.

The QED radiative corrections contribute to the hyperfine structure at a level that is significant and should be taken into account in high-accuracy calculations. Indeed, the corrections for ^{133}Cs and ^{135}Ba$^+$ are both -0.38%, while the overall deviation of our theoretical determination of the hyperfine structure is 0.17% for Cs and 0.21% for Ba$^+$ (excluding Bohr-Weisskopf uncertainties). The QED radiative corrections increase with nuclear charge and contribute -0.61% and -0.57% to the hyperfine intervals for ^{211}Fr and ^{225}Ra$^+$, respectively.

We note that for reliable determination of the QED radiative corrections to the hyperfine structure, rigorous calculations are required. In Ref. [63], for example, a "radiative potential" was used for estimation of the QED effects for the hyperfine structure. They obtained results for Ba$^+$, Cs, Fr, and Ra$^+$ that are more than a factor of two larger than those found in the current work and Ref. [19]. A radiative potential—see, e.g., Refs. [9,13]—may be used reliably for determination of radiative corrections to binding energies and other observables where the largest part of the correction arises from perturbations to the wave functions (e.g., E1 amplitudes). However, for the hyperfine structure and other short-distance operators, there is no reason that the vertex diagrams should be small.

We have shown that for heavier nuclei the effect of the finite magnetization distribution becomes increasingly important. In particular, for ^{211}Fr and ^{225}Ra$^+$, its contribution is several times larger than the QED radiative corrections (by as much as eight times for ^{225}Ra$^+$). Moreover, the uncertainty due to the lack of knowledge of the magnetization distribution for heavier nuclei completely masks the QED radiative corrections, similar to the case for hydrogenlike ions [54]. For ^{133}Cs and ^{135}Ba$^+$, the Bohr-Weisskopf uncertainty limits the test of the electronic wave functions by several 0.1%. For ^{225}Ra$^+$, this uncertainty is estimated to be 1.4%, strongly limiting a high-precision test of many-electron wave functions in hyperfine structure studies. Furthermore, for ^{211}Fr, the 2% uncertainty in the value for the nuclear magnetic moment prohibits an accurate test.

Depending on the nuclear spin and parity, we emphasise that the Bohr-Weisskopf effect may be very different when different magnetization models are considered. In particular,

we have seen for ^{133}Cs that the single-particle model yields a value that is several times smaller than the sphere. The result for the ground-state hyperfine splitting changes by as much as 0.5% when we move from the sphere model (commonly used in hyperfine calculations for this atom) to the more well-motivated nuclear single-particle model.

VII. CONCLUSION

We have performed rigorous calculations of the one-loop QED radiative corrections to the hyperfine structure intervals for atoms and ions of interest for parity violation studies. These corrections contribute −0.24% (^{87}Rb), −0.38% (^{133}Cs), −0.38% (^{135}Ba$^+$), −0.61% (^{211}Fr), and −0.57% (^{225}Ra$^+$) and should be included in accurate theoretical determinations of the hyperfine structure. We have also studied the Bohr-Weisskopf correction employing different nuclear magnetization distribution models and estimated its uncertainty. We have found that this uncertainty grows with nuclear charge and strongly impedes the ability to accurately probe the correlation and QED effects. We have completed our hyperfine structure analysis with full many-body calculations performed in the all-orders correlation potential method.

This work is a step towards an improved theoretical understanding of the hyperfine structure for heavy atoms and ions. It demonstrates the need for control of the nuclear physics uncertainties before accurate tests (at the level of 0.1%) of the electronic wave functions in the nuclear region may be made using hyperfine interval comparisons.

ACKNOWLEDGMENTS

J.S.M.G. is grateful to V. Dzuba for providing the structural radiation codes and for useful discussions. J.S.M.G. is grateful to Helmholtz-Institut Jena for kind hospitality over a three-month visit and also acknowledges support from UNSW Sydney where she was based at the start of this project. This work was supported by the Australian Research Council through the Centre of Excellence in Engineered Quantum Systems (EQuS), Project No. CE110001013.

[1] C. S. Wood, S. C. Bennett, D. Cho, B. P. Masterson, J. L. Roberts, C. E. Tanner, and C. E. Wieman, Science **275**, 1759 (1997).
[2] O. P. Sushkov, Phys. Rev. A **63**, 042504 (2001).
[3] W. R. Johnson, I. Bednyakov, and G. Soff, Phys. Rev. Lett. **87**, 233001 (2001).
[4] M. Yu. Kuchiev and V. V. Flambaum, Phys. Rev. Lett. **89**, 283002 (2002).
[5] A. I. Milstein, O. P. Sushkov, and I. S. Terekhov, Phys. Rev. Lett. **89**, 283003 (2002).
[6] J. Sapirstein, K. Pachucki, A. Veitia, and K. T. Cheng, Phys. Rev. A **67**, 052110 (2003).
[7] V. M. Shabaev, K. Pachucki, I. I. Tupitsyn, and V. A. Yerokhin, Phys. Rev. Lett. **94**, 213002 (2005).
[8] V. M. Shabaev, I. I. Tupitsyn, K. Pachucki, G. Plunien, and V. A. Yerokhin, Phys. Rev. A **72**, 062105 (2005).
[9] V. V. Flambaum and J. S. M. Ginges, Phys. Rev. A **72**, 052115 (2005).
[10] J. S. M. Ginges and V. V. Flambaum, Phys. Rep. **397**, 63 (2004).
[11] L. Labzowsky, I. Goidenko, M. Tokman, and P. Pyykkö, Phys. Rev. A **59**, 2707 (1999).
[12] J. Sapirstein and K. T. Cheng, Phys. Rev. A **66**, 042501 (2002).
[13] V. M. Shabaev, I. I. Tupitsyn, and V. A. Yerokhin, Phys. Rev. A **88**, 012513 (2013).
[14] C. Thierfelder and P. Schwerdtfeger, Phys. Rev. A **82**, 062503 (2010).
[15] B. M. Roberts, V. A. Dzuba, and V. V. Flambaum, Phys. Rev. A **87**, 054502 (2013).
[16] J. S. M. Ginges and J. C. Berengut, Phys. Rev. A **93**, 052509 (2016).
[17] J. Sapirstein and K. T. Cheng, Phys. Rev. A **71**, 022503 (2005).
[18] B. K. Sahoo and B. P. Das, Mol. Phys. **115**, 2765 (2017).
[19] J. Sapirstein and K. T. Cheng, Phys. Rev. A **67**, 022512 (2003).
[20] J. Sapirstein and K. T. Cheng, Phys. Rev. A **78**, 022515 (2008).
[21] D. Antypas and D. S. Elliott, Phys. Rev. A **87**, 042505 (2013).
[22] E. Gomez, L. A. Orozco, and G. D. Sprouse, Rep. Prog. Phys. **69**, 79 (2006).
[23] E. Gomez, S. Aubin, R. Collister, J. A. Behr, G. Gwinner, L. A. Orozco, M. R. Pearson, M. Tandecki., D. Sheng, and J. Zhang, J. Phys. Conf. Series **387**, 012004 (2012).
[24] M.-A. Bouchiat, Phys. Rev. Lett. **100**, 123003 (2008).
[25] N. Fortson, Phys. Rev. Lett. **70**, 2383 (1993).
[26] T. W. Koerber, M. Schacht, W. Nagourney, and E. N. Fortson, J. Phys. B **36**, 637 (2003).
[27] M. Nuñez Portela, E. A. Dijck, A. Mohanty, H. Bekker, J. E. van den Berg, G. S. Giri, S. Hoekstra, C. J. G. Onderwater, S. Schlesser, R. G. E. Timmermans, O. O. Versolato, L. Willmann, H. W. Wilschut, and K. Jungmann, Appl. Phys. B **114**, 173 (2014).
[28] V. A. Dzuba, V. V. Flambaum, and B. Roberts, Phys. Rev. A **86**, 062512 (2012).
[29] W. J. Marciano and J. L. Rosner, Phys. Rev. Lett. **65**, 2963 (1990).
[30] V. Cirigliano and M. J. Ramsey-Musolf, Prog. Part. Nucl. Phys. **71**, 2 (2013).
[31] J. Erler and S. Su, Prog. Part. Nucl. Phys. **71**, 119 (2013).
[32] V. A. Dzuba, V. V. Flambaum, and J. S. M. Ginges, Phys. Rev. D **66**, 076013 (2002).
[33] S. G. Porsev, K. Beloy, and A. Derevianko, Phys. Rev. Lett. **102**, 181601 (2009).
[34] V. A. Dzuba, J. C. Berengut, V. V. Flambaum, and B. Roberts, Phys. Rev. Lett. **109**, 203003 (2012).
[35] V. A. Dzuba, V. V. Flambaum, and I. B. Khriplovich, Z. Phys. D **1**, 243 (1986).
[36] E. N. Fortson, Y. Pang, and L. Wilets, Phys. Rev. Lett. **65**, 2857 (1990).
[37] M. J. Ramsey-Musolf, Phys. Rev. C **60**, 015501 (1999).
[38] W. Kohn and L. J. Sham, Phys. Rev. **140**, A1133 (1965).
[39] R. Latter, Phys. Rev. **99**, 510 (1955).
[40] I. Angeli and K. P. Marinova, At. Data Nucl. Data Tables **99**, 69 (2013).
[41] N. J. Stone, At. Data Nucl. Data Tables **90**, 75 (2005).
[42] A. Bohr and V. F. Weisskopf, Phys. Rev. **77**, 94 (1950).

[43] A. V. Volotka, D. A. Glazov, G. Plunien, and V. M. Shabaev, Ann. Phys. **525**, 636 (2013).
[44] J. Sapirstein and K. T. Cheng, Phys. Rev. A **74**, 042513 (2006).
[45] V. M. Shabaev, Phys. Rep. **356**, 119 (2002).
[46] A. V. Volotka, D. A. Glazov, I. I. Tupitsyn, N. S. Oreshkina, G. Plunien, and V. M. Shabaev, Phys. Rev. A **78**, 062507 (2008).
[47] A. V. Volotka, D. A. Glazov, V. M. Shabaev, I. I. Tupitsyn, and G. Plunien, Phys. Rev. Lett. **103**, 033005 (2009).
[48] D. A. Glazov, A. V. Volotka, V. M. Shabaev, I. I. Tupitsyn, and G. Plunien, Phys. Rev. A **81**, 062112 (2010).
[49] P. J. Mohr, G. Plunien, and G. Soff, Phys. Rep. **293**, 227 (1998).
[50] O. V. Andreev, D. A. Glazov, A. V. Volotka, V. M. Shabaev, and G. Plunien, Phys. Rev. A **85**, 022510 (2012).
[51] A. N. Artemyev, V. M. Shabaev, G. Plunien, G. Soff, and V. A. Yerokhin, Phys. Rev. A **63**, 062504 (2001).
[52] M. Le Bellac, Nucl. Phys. **40**, 645 (1963).
[53] V. M. Shabaev, J. Phys. B **27**, 5825 (1994).
[54] V. M. Shabaev, M. Tomaselli, T. Kühl, A. N. Artemyev, and V. A. Yerokhin, Phys. Rev. A **56**, 252 (1997).
[55] J. Zhang, M. Tandecki, R. Collister, S. Aubin, J. A. Behr, E. Gomez, G. Gwinner, L. A. Orozco, M. R. Pearson, and G. D. Sprouse, Phys. Rev. Lett. **115**, 042501 (2015).
[56] V. A. Dzuba, V. V. Flambaum, P. G. Silvestrov, and O. P. Sushkov, J. Phys. B **20**, 1399 (1987).
[57] W. R. Johnson, *Atomic Structure Theory*, Lectures on Atomic Physics (Springer, Berlin, 2007).
[58] E. Arimondo, M. Inguscio, and P. Violino, Rev. Mod. Phys. **49**, 31 (1977).
[59] W. Becker, R. Blatt, and G. Werth, J. Phys. (Paris) **42**, C8-339 (1981).
[60] J. E. Sansonetti, J. Phys. Chem. Ref. Data **36**, 497 (2007).
[61] U. Dammalapati, K. Jungmann, and L. Willmann, J. Phys. Chem. Ref. Data **45**, 013101 (2016).
[62] V. A. Dzuba, V. V. Flambaum, P. G. Silvestrov, and O. P. Sushkov, Phys. Lett. A **131**, 461 (1988).
[63] T. H. Dinh, V. A. Dzuba, and V. V. Flambaum, Phys. Rev. A **80**, 044502 (2009).